

RESEARCH ARTICLE

# Statistical Modeling Applied to Deformation-Relaxation Processes in a Composite Biopolymer Network Induced by Magnetic Field

Javier Tarrío-Saavedra<sup>1</sup>, Cécilia Galindo González<sup>2</sup>, Salvador Naya<sup>1</sup>, Jorge López-Beceiro<sup>3</sup>, Alain Ponton<sup>2\*</sup>

**1** Department of Mathematics, EPS. University of A Coruña. Avda. Mendizábal s/n. Ferrol. Spain, **2** Matière et Systèmes Complexes CNRS, UMR 7057, Université Paris Diderot-Paris 7 Bâtiment Condorcet Case 7056, Paris, **3** Department of Industrial Engineering II, EPS. University of A Coruña. Avda. Mendizábal s/n. Ferrol. Spain

\* [alain.ponton@univ-paris-diderot.fr](mailto:alain.ponton@univ-paris-diderot.fr)



**OPEN ACCESS**

**Citation:** Tarrío-Saavedra J, González CG, Naya S, López-Beceiro J, Ponton A (2017) Statistical Modeling Applied to Deformation-Relaxation Processes in a Composite Biopolymer Network Induced by Magnetic Field. PLoS ONE 12(1): e0169866. doi:10.1371/journal.pone.0169866

**Editor:** Jeffrey Chalmers, The Ohio State University, UNITED STATES

**Received:** March 23, 2016

**Accepted:** December 23, 2016

**Published:** January 12, 2017

**Copyright:** © 2017 Tarrío-Saavedra et al. This is an open access article distributed under the terms of the [Creative Commons Attribution License](https://creativecommons.org/licenses/by/4.0/), which permits unrestricted use, distribution, and reproduction in any medium, provided the original author and source are credited.

**Data Availability Statement:** All relevant data are within the paper.

**Funding:** This research has been supported by the Spanish Ministry of Science and Innovation Grant MTM2014-52876-R (ERDF included).

**Competing Interests:** The authors have declared that no competing interests exist.

## Abstract

This study investigated a methodology based on image processing and statistics to characterize and model the deformation upon controlled and uniform magnetic field and the relaxation under zero field of droplets observed in aqueous solutions of sodium alginate incorporating magnetic maghemite nanoparticles stabilized by adsorption of citrate ions. The changes of droplet geometry were statistically analyzed using a new approach based on the data obtained from optical microscopy, image processing, nonlinear regression, evolutionary optimization, analysis of variance and resampling. Image enhancement and then image segmentation (Gaussian mixture modeling) processes were applied to extract features with reliable information of droplets dimensions from optical micrographs. The droplets deformation and relaxation trends were accurately adjusted by the Kohlrausch-Williams-Watts (KWW) function and a mean relaxation time was obtained by fitting the time evolution of geometry parameters. It was found to be proportional to the initial radius of the spherical droplets and was associated to interfacial tension.

## Introduction

Nanocomposite materials composed of a polymer network in the presence of particles is nowadays a subject of intensive research due to the possibility to modulate their mechanical [1], optical, thermal [1–4], sound, magnetic, electric properties. Indeed these complex materials are potentially attractive to the development of many technologies such as electronics, optics, sensors, actuators, drug delivery and many other biotechnological areas.

Nanoparticles of different nature (gold, silver, iron, cobalt, nickel, copper, alloys, metal-derived quantum dots) can be incorporated into polymer network [5].

A special attention has been paid to magnetic nanoparticles to elaborate novel magnetoresponsive composites whose physical properties can be controlled by applying external

magnetic field. In this case macroscopic behaviour is impacted by magnetic induced chain like or clustering structures. Thus, the study of microstructure is of decisive importance in order to get a better knowledge of these magnetoresponse composites [6].

In this work, we propose a new methodology to study the deformation of magnetic field induced droplets and their relaxation when the magnetic field is switched off in an aqueous solution of biopolymer. For this purpose image enhancement techniques and an image segmentation procedure were applied to obtain data on size and shape changes of droplets. Then characteristic time of deformation and relaxation processes was obtained by a nonlinear parametric regression model as proposed by Kohlrausch, Williams and Watts (KKW) [7].

The experimental conditions are presented in the second section. The image processing techniques applied in the present study are introduced in the third section. In the fourth, the design of experiments is described while in the fifth one the results are shown and discussed before final conclusions in the sixth section.

## Experimental

### Materials

The biopolymer was a polysaccharide extracted from marine brown algae, the alginic acid (Alginate). It is a linear copolymer containing  $\beta$ -1,4-D-mannuronate (M) and  $\alpha$ -1,4-L-guluronate (G) units in various proportions and sequences depending on the season, age and the part of the plant used for extraction. With one carboxylate group in each M or G unit, alginate is a highly negatively charged polyelectrolyte at neutral or basic pH. Dissolving in water, the sodium ions and the carboxylate groups of the alginate are ionized to form the alginate polyelectrolyte and to deliver sodium ions in the medium.

The used ferrofluid was an aqueous solution of ferromagnetic nanoparticles of maghemite ( $\gamma$ - $\text{Fe}_2\text{O}_3$ ) prepared by alkaline coprecipitation of ferric and ferrous salts in water [8]. Concentrated ammonium hydroxide is added to an acidic solution of iron (II) chloride and iron (III) chloride leading to the precipitation of anionic magnetite ( $\text{Fe}_3\text{O}_4$ ) particles. After washing with distilled water, they are stirred in nitric acid, oxidized into maghemite ( $\gamma$ - $\text{Fe}_2\text{O}_3$ ) by a boiling solution of ferric nitrate and washed with acetone. These nanoparticles coated with hydroxo ligands are spontaneously soluble in aqueous acidic solutions at pH  $\sim 2$  with  $\text{NO}_3^-$  counterions. Firstly in water, the surface can be coated with citrate ligands in order to obtain dispersions at pH  $\sim 7$ . This coating is obtained by adding trisodium citrate to the native acidic ferrofluid ( $[\text{Cit}]/[\text{iron}] = 0.1$ ), which is heated at  $90^\circ\text{C}$  during 10 minutes. After several washings with water/acetone mixtures, a stable citrated ferrofluid with pH close to 7 is obtained.

The magnetic properties are determined by magnetization  $M$  measurements on stable dispersions under an applied magnetic field  $H$ , ranging between 0 and 800 kA/m, at room temperature with a home-made vibrating magnetometer. High field determination of  $M_{\text{HF}}$  in the saturation region allows us to determine the saturation magnetization  $M_S$  of the nanoparticles of volume fraction  $\Phi$  as  $M_S = M_{\text{HF}}/\Phi$ . In all samples here, the size distribution of the nanoparticles can be described by a lognormal distribution of diameters with the same median diameter  $d_0 \sim 7$  nm (with  $\ln d_0 = \langle \ln d \rangle$ ) and a polydispersity index  $\sigma$  between 0.3 and 0.4 with a saturation magnetization  $M_S = 310 \pm 25$  kA/m.

### Sample preparation

A solution of sodium alginate (concentration  $C_{\text{alg}} = 18$  g.L $^{-1}$ ) was first prepared by mixing sodium alginate powder in distilled water with mechanical stirring at a speed of 400 rpm during 18 hours at room temperature.

The mixture was then obtained by introducing the ferrofluid (volume fraction of nanoparticles ( $\Phi_{NP} = 1\%$ ) in the previous aqueous sodium alginate solution.

### Characterization methods

Optical microscopy observation was carried out using a laboratory made special device allowing the application of a magnetic field during the observations. Two moving permanent magnets were placed in slots of a non-magnetic circular plate (Fig 1). A rectangular capillary filled with sodium alginate solutions incorporating citrated ferrofluids was placed at the middle of the plate perpendicularly to the direction of the magnetic field. The capillary was closed on both ends by modeling clay to avoid evaporation. The observation was performed by a Nikon

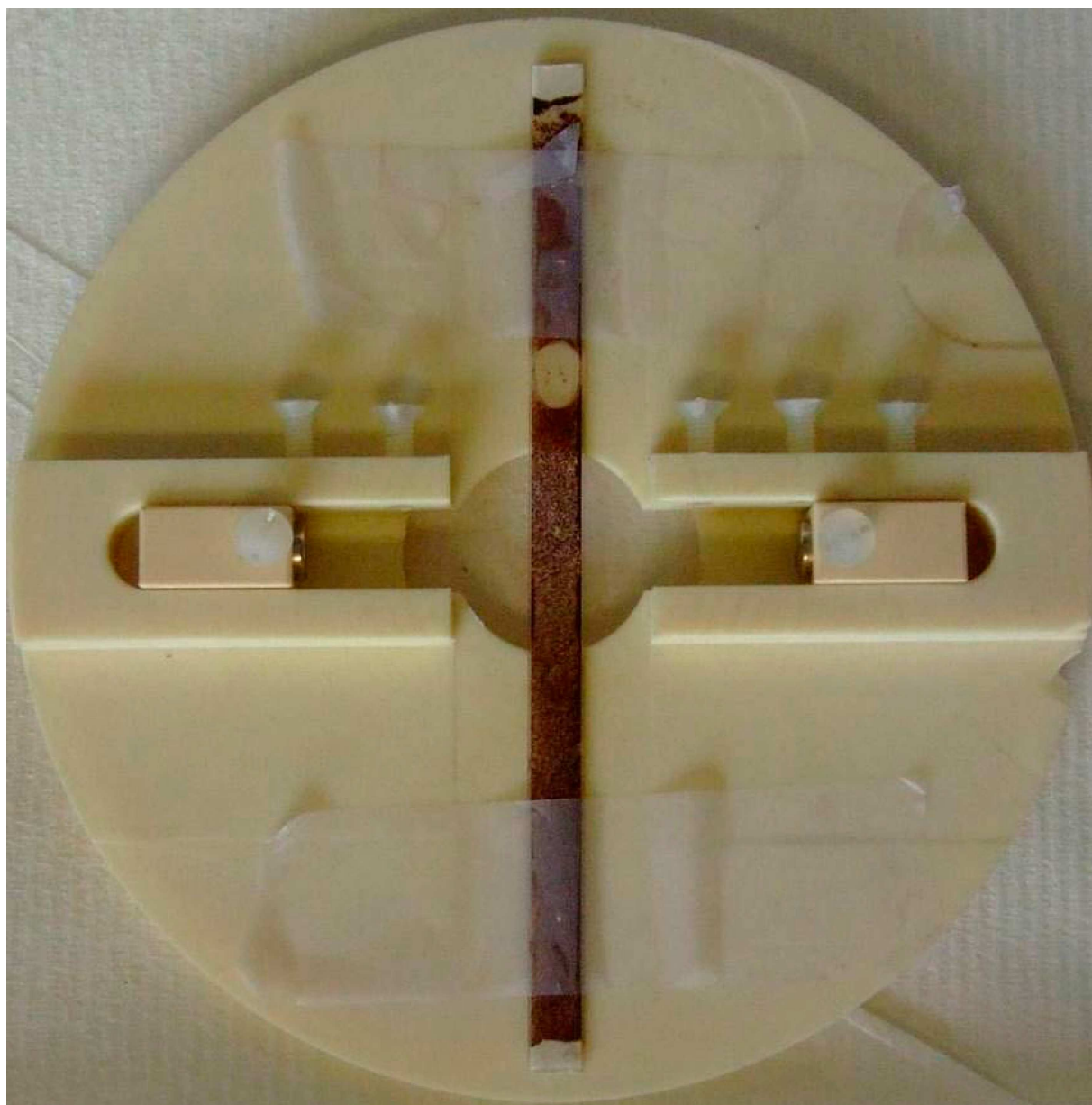


**Fig 1. Home-made device for optical observation under application of magnetic field.**

doi:10.1371/journal.pone.0169866.g001

microscope with a magnification objective of 10x at one value of magnetic field strength ( $3.2 \text{ kA m}^{-1}$ ). The magnetic field was applied for 5 minutes before recording images analyzed by freeware software.

### Image processing and features extraction

The application of image processing analysis was necessary to extract the droplets geometrical information from the optical micrographs. Fig 2 shows the scheme of the proposed image processing procedure that was previously used in material classification and identification tasks such as wood species [9]. This procedure provides an alternative way to collect information about relaxation processes in magnetic droplets within polymeric solutions. Image analysis application allows to extract a vector of representative features related to the geometry of the objects in the image such as diameter, area, distance, circularity, rectangularity, position, etc. [9]. ImageJ [10] and R software (through biOps library) [11] free software programs have been used to implement the enhancement and segmentation tasks (Fig 2). It is also important to note that these processes were optimized for each one of the studied droplets.

### Image enhancement

The obtained micrographs require the application of a set of image enhancement techniques in order to remove their noise and enhance their contrast. Noise is the random information variation of color and brightness and it may be attenuated applying some enhancement tools named filters, such as the well-known median filter [12]. In addition, the histogram

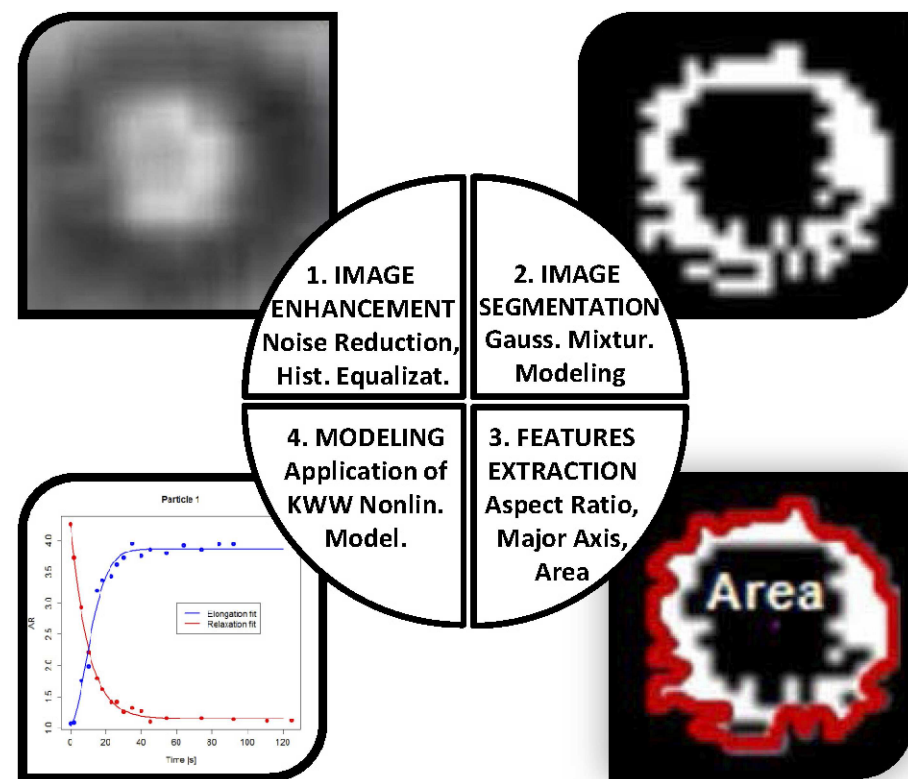


**Fig 2. Proposed methodology scheme for studying the relaxation processes of magnetic droplets under the application of a weak magnetic field.**

doi:10.1371/journal.pone.0169866.g002

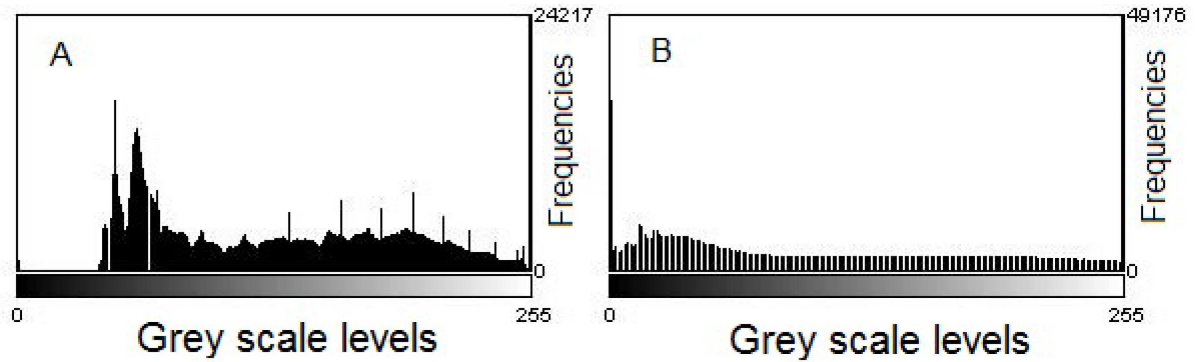


**Fig 3. Histogram equalization procedure applied to a droplet micrograph.** A: intensity histogram before the equalization process. B: intensity histogram after the application of histogram equalization process.

doi:10.1371/journal.pone.0169866.g003

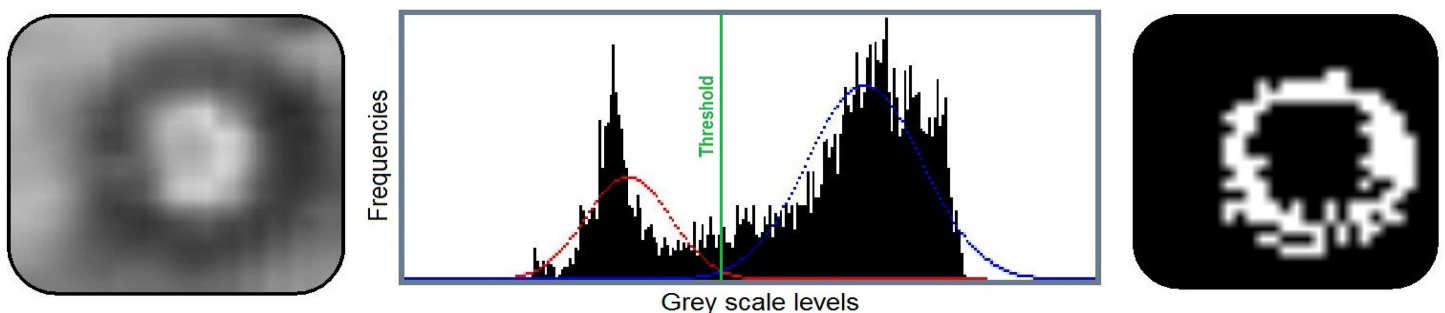
equalization technique was used to improve the image contrast, i.e. a uniform intensity histogram is obtained, by applying a monotonic and nonlinear mapping (see Fig 3)

### Image segmentation

The image segmentation is a process for splitting a digital image into several groups of pixels, in this case two (black and white), so that the geometry of the droplets is clearly observed. The segmentation procedure is composed of three main steps. Estimating the brightness limit value that distinguishes objects (in this case magnetic droplets) from the background in the thresholding task, to identify the points where the brightness abruptly changes by edge detection (e.g. using Sobel operator [9]) and, finally, obtain continuous edges by applying a dilation process.

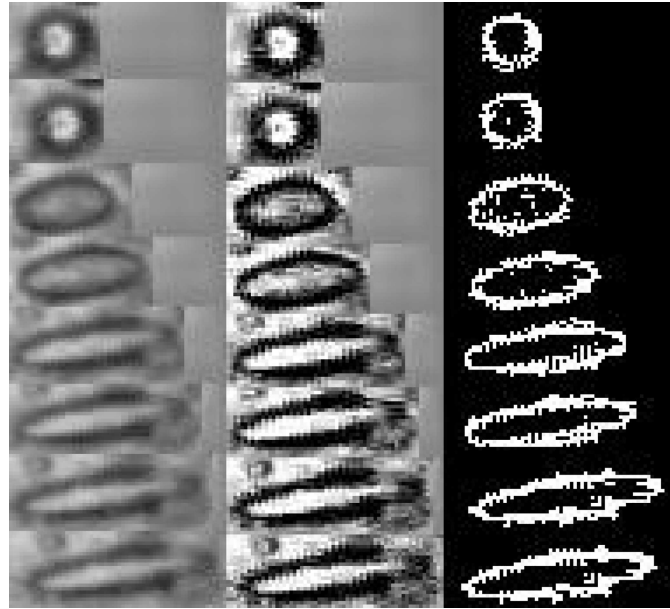
In the present paper, the Gaussian Mixture Modeling algorithm was used for obtaining the threshold value used in the segmentation process [13]. This algorithm separates the histogram of an image into two classes by calculating the image threshold as the intersection of these two Gaussian distributions, as shown in Fig 4. This thresholding technique allows to distinguish the droplets from the background by including (in addition to threshold estimation) a grey-scale binning process and an image inversion step (see Fig 5).

Fig 5 shows the image processing sequence corresponding to a studied droplet at the times 0, 2, 6, 10, 15, 18, 23 and 26 s of application of a low magnetic field: the first column represents the original images obtained using an optical microscope, the second one shows the images



**Fig 4. Gaussian Mixture Modeling process of segmentation applied to a droplet micrograph.** Left panel: enhanced micrograph. Center: intensity histogram where two Gaussian distribution are fitted, in blue and red. Right: resulting segmented micrographs.

doi:10.1371/journal.pone.0169866.g004



**Fig 5. Image processing sequence corresponding to a studied droplet under the applied magnetic field.**

doi:10.1371/journal.pone.0169866.g005

after the enhancement process and the third one corresponds to the result of the segmentation process.

### Features extraction

After the segmentation process we have obtained connected objects, in this case they represent the magnetic droplets. Three characteristics related to the geometry of the droplets are extracted from the segmented images: (i) major diameter (major) corresponding to an ellipse that fit each droplet, measured in micrometer,  $\mu\text{m}$ , (ii) droplet area calculated by numerical methods and measured using squared micrometers,  $\mu\text{m}^2$ , (iii) aspect ratio (AR), the ratio between the major and the minor diameter of the ellipse fitted to each droplet. The goal is to obtain representative features of droplets geometry, that may summarize their shape and size of droplets, in order to monitor the changes of droplet geometry depending on time during the application of magnetic field, and then when the magnetic field is switched off.

### Design of Experiments and Data Collection

The deformation of droplets under application of a constant value ( $3.2 \text{ kA m}^{-1}$ ) of magnetic field and their relaxation under zero magnetic field are illustrated on Figs 6 and 7, respectively. It should be noted that droplets tend to interact with each other changing their geometrical dimensions. Droplets aggregation or disaggregation can be observed in addition to pure magnetic deformation/relaxation of individual droplets leading to the absence of mass conservation. Consequently, in order to study only the geometrical changes due to magnetic field application, 5 different droplets, of different sizes, that do not interact with the surrounding droplets were finally chosen from images. Taking into account that the most droplets interact with the others, changing their size and shape, the chosen 5 droplets is a representative sample of the overall number of droplets where there is no aggregation, disaggregation or other interaction with the surrounding area (Fig 8).

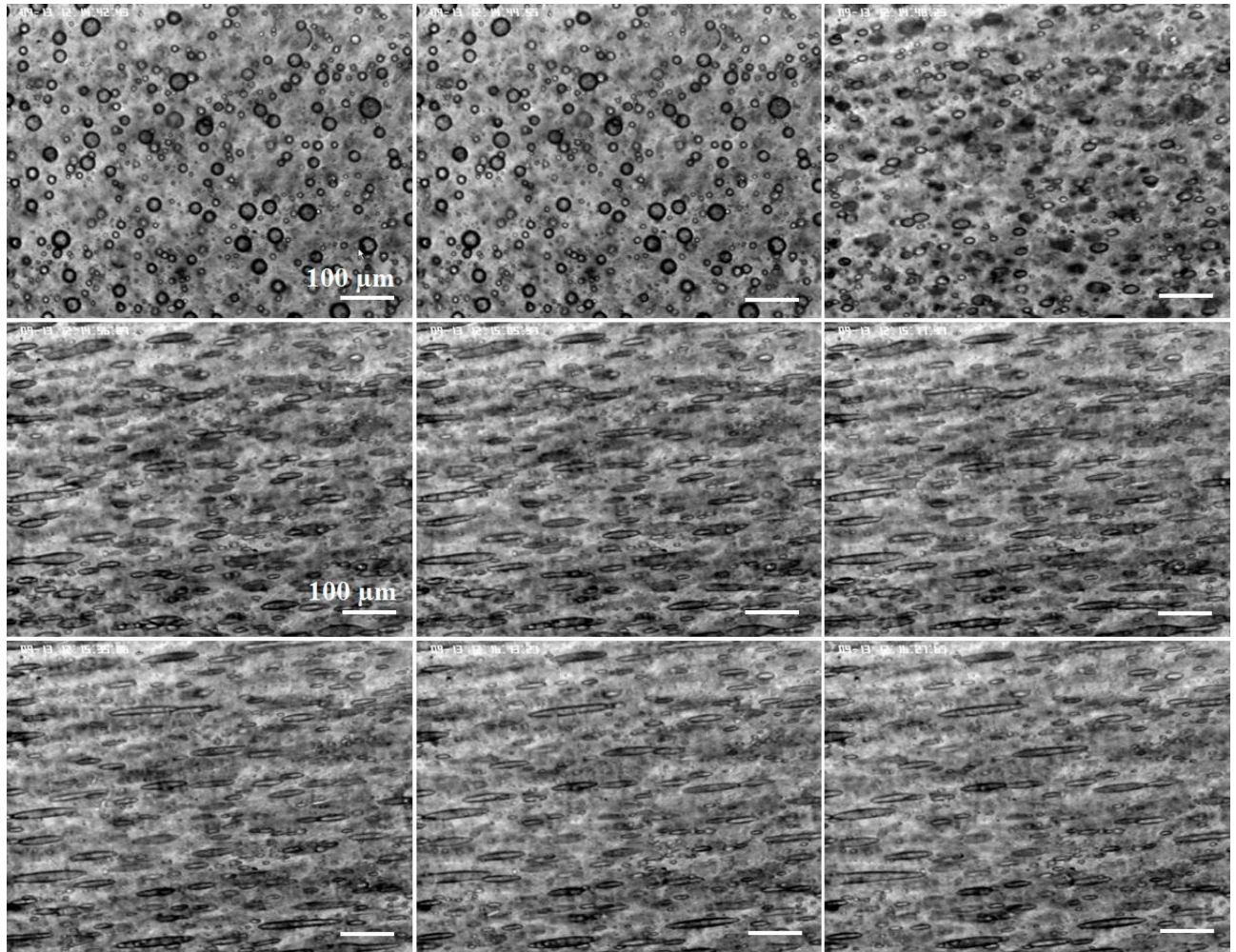


**Fig 6.** From left to right and from top to bottom, deformation of droplets under a constant value of magnetic field (3.2 kA/m) at different times 0, 6, 15, 23, 35, 45, 54, 92 and 106 s. The scale is the same for all the micrographs.

doi:10.1371/journal.pone.0169866.g006

As mentioned in section 3, three different geometrical parameters were measured: area, AR, and major diameter of the ellipse that fits each droplet. In addition, we separated the measures corresponding to elongation and dimension recovery processes for each droplet. Finally, the droplet dimensions corresponding to each time were calculated attending to three variables defined as factors, applying the image analysis techniques mentioned in the next section. These three factors are the studied “droplet” (with five levels, each one corresponding to each droplet), the selected “geometric measure” (at three levels: area, AR and major diameter) and the “change of dimension process” suffered by each droplet (elongation or dimension recovery).

We want to test if the droplet geometrical changes depend on the “droplet”, “geometric measure”, and “change of dimension process” (are the magnetic induced geometric changes reversible?). Therefore, it is necessary to apply statistical design of experiments (DOE) techniques as analysis of variance (ANOVA), using F and Tukey tests [14, 15], and even multivariate analysis of variance (MANOVA). These procedures were successfully implemented in a wide range of applications [16–20].

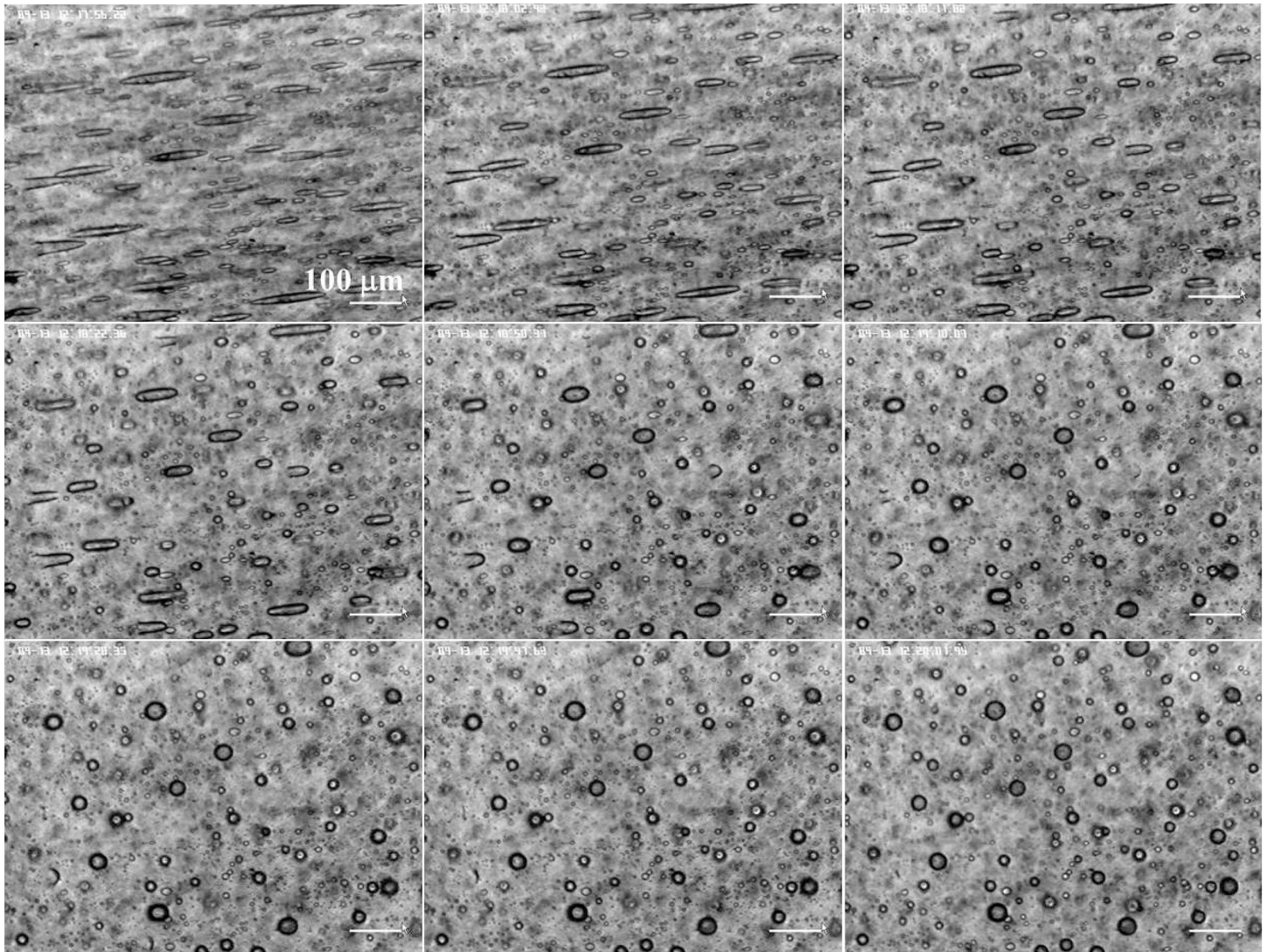


**Fig 7.** From left to right and from top to bottom, relaxation of droplets when the magnetic field is switched off at different times, at 0, 6, 15, 26, 54, 74, 92, 111 and 125 s. The scale is the same for all the micrographs.

doi:10.1371/journal.pone.0169866.g007

Statistical DoE are usually performed for testing which factors or quantitative variables affect to the response variable. This response variable is a continuous variable or a vector composed of several ones. In the case of univariate response, the ANOVA is implemented, using F test to statistically infer if at least one level of the factor produces significant changes in the continuous response [14]. The Tukey test is also used to perform pairwise comparisons, i. e. to discern which factor levels produces those significant differences in the response [15]. Otherwise, concerning the multivariate response, the multivariate analysis of variance (MANOVA) with Pillai test [21, 22] was applied.

Therefore, two different models of analysis of variance, characterized by the type of response, were performed for testing the impact of each studied factor on the geometry of droplets (and thus on their relaxation processes).

On the one hand, in the MANOVA model, the response is multivariate and corresponds to the KWW nonlinear function parameters  $(a, b, \lambda_c, \beta)$  vector [23]. This vector represents a



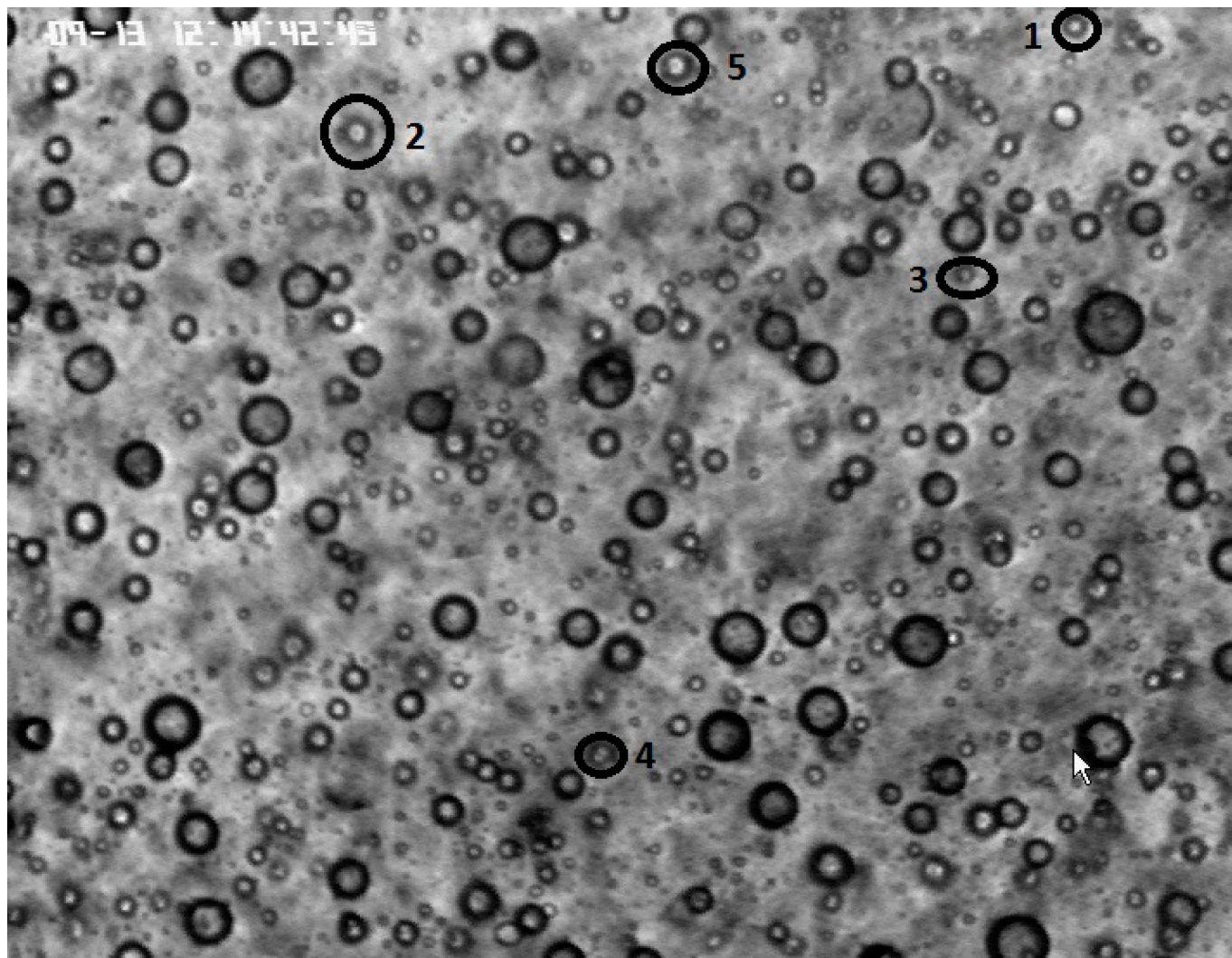


**Fig 8. Magnetic droplets selected in the present study where neither disaggregation nor aggregation takes place.**

doi:10.1371/journal.pone.0169866.g008

sequence of features that summarize the information of each dimensional curve, where the AR, major diameter and area values are plotted versus the time of magnetic field application. Thus, whether differences in features vectors are statistically detected, we can infer that there will be differences in the compared geometrical curves. The MANOVA is developed, applying the Pillai test [21, 22] for checking the influence of both the multivariate response ( $a$ ,  $b$ ,  $\lambda_c$ ,  $\beta$ ) KWW parameters vector [23]) and three factors: (i) “Droplet”, at five levels named: 1, 2, 3, 4 and 5; (ii) Geometric measure or “magnitude”, at three levels: area, AR and major diameter; (iii) change of dimension process” at two levels: droplet elongation and dimension recovery.

On the other hand, the second analysis of variance model is focused only on the characteristic relaxation times ( $\lambda_c$ ) obtained from each estimated KWW nonlinear equation. The aim is to focus the analysis only in characteristic relaxation time estimation, the most informative parameter of KWW model. Thus, an ANOVA model is performed to analyse the univariate response (the response variable is the  $\lambda_c$  obtained by the application of KWW model) and the same three factors as above for MANOVA:

### Results and Discussion

The time dependence of AR for the 5 droplets under applied magnetic field (deformation) and when the magnetic field is switched off (relaxation) is presented on Fig 9A and 9B respectively. Similar behaviours were observed for major diameter and area of droplets. Then, experimental data were fitted by the KWW nonlinear regression model corresponding to each different “droplet” and “change of dimension process”,  $AR(t)$  or Major diameter  $(t)$  or Area  $(t) = a + b \exp(-t/\lambda_c)^\beta$  where  $a$  is the initial value of the measured geometrical dimension,  $b$  is the equivalent to the instantaneous modulus in the case of viscoelastic properties,  $\beta$  is related to the width of the distribution of relaxation time and  $\lambda_c$  currently corresponds to a characteristic relaxation time. The value  $\beta = 1$  corresponds to a monoexponential relaxation process with an unique relaxation time.

Optimum fittings were obtained by applying the Differential Evolution evolutionary global optimization algorithm (DE), through the DEoptim function of the R DEoptim package [24, 25]. The KWW parameters ( $a, b, \lambda_c, \beta$ ) obtained from fittings corresponding to the 3 geometrical indexes of the droplets are given in Table 1.

The good fittings of experimental data are attested by the values of the determination coefficients ( $R^2$ ) [14]. Whatever the geometrical parameter (area, AR or major diameter), it could be observed that the characteristic relaxation time  $\lambda_c$  is in the same order of magnitude for the deformation and relaxation of droplets indicating a reversibility of the process. There is only

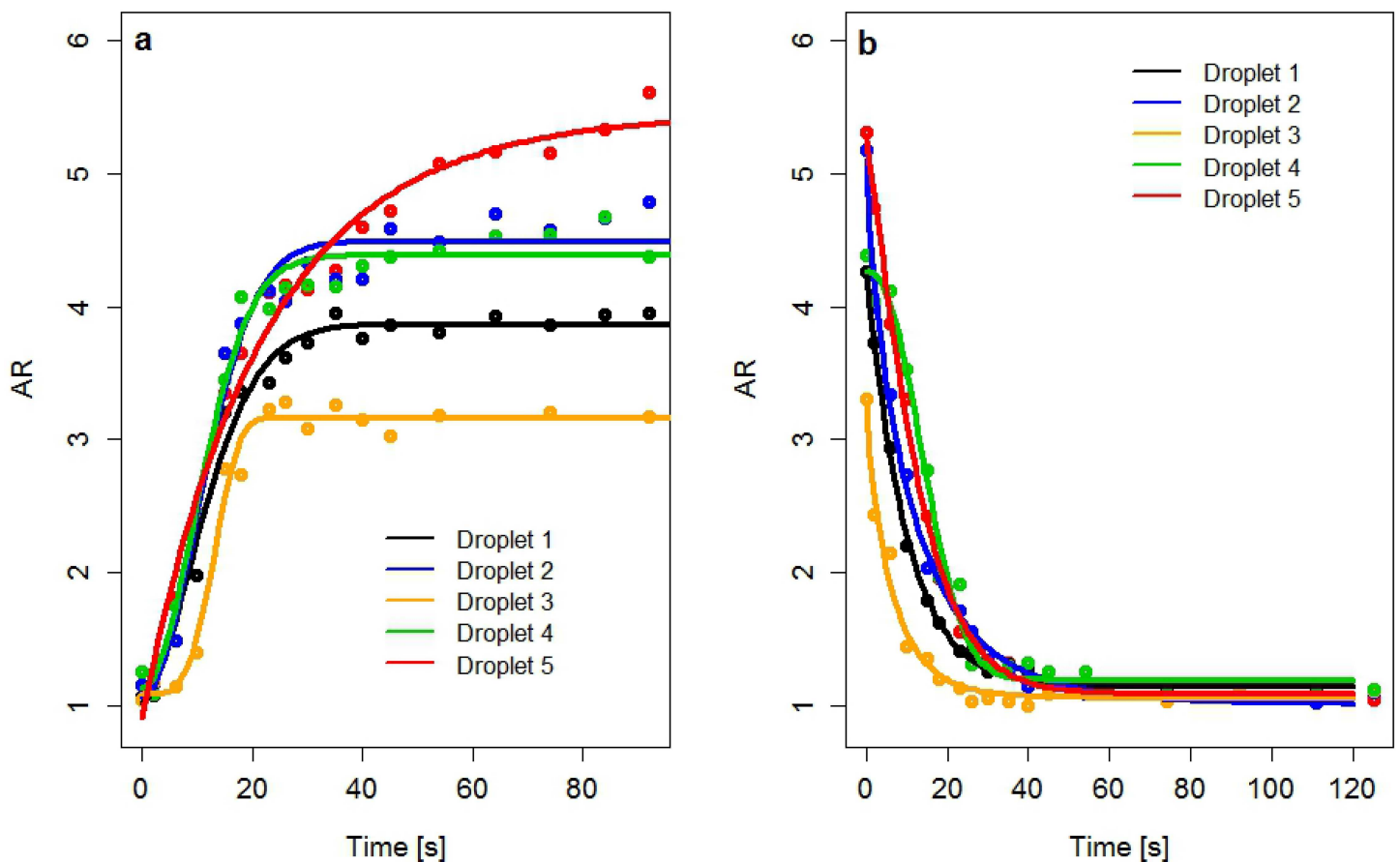


**Fig 9.** Time dependence of the AR of the 5 droplets under magnetic field (a) and when the magnetic field is switched off (b). The solid lines correspond to the fitting of experimental data by KWW nonlinear model, using the DE Algorithm.

doi:10.1371/journal.pone.0169866.g009

**Table 1. KWW model parameters and R<sup>2</sup> coefficients obtained applying DE optimization algorithm for each combination of the three factors.** The unit of a depends on the geometric variable (area, major diameter, aspect ratio).

Elongation process					Dimension recovery process					Geom. Variable	Droplet
a [μm <sup>2</sup> ] or [μm] or []	b	λ <sub>c</sub> [s]	β	R <sup>2</sup>	a [μm <sup>2</sup> ] or [μm] or []	b	λ <sub>c</sub> [s]	β	R <sup>2</sup>		
176.1	68.13	13.22	1.31	0.90	281.9	-114.8	10.16	1.22	0.97	Area	1
319.1	320.1	16.22	2.24	1.00	641.5	-330.2	13.15	1.68	1.00	Area	
112.5	138.8	7.980	1.13	0.98	232.2	-121.8	4.560	2.04	0.94	Area	3
285.2	203.7	14.59	2.02	0.96	492.7	-195.7	12.49	4.95	0.98	Area	4
322.1	333.7	13.12	1.29	0.99	675.3	-428.4	9.520	1.38	0.98	Area	5
1.15	3.126	9.873	1.04	0.99	3.87	-2.837	13.930	1.69	0.89	AR	1
1.02	4.081	11.02	0.82	0.98	4.49	-3.417	14.121	1.91	0.99	AR	2
1.06	2.197	6.325	0.89	0.98	3.16	-2.072	14.217	4.10	0.98	AR	3
1.20	3.068	17.34	2.30	0.98	4.38	-3.244	13.515	1.94	0.99	AR	4
1.09	4.145	13.23	1.22	0.99	5.44	-4.528	22.019	0.984	1.00	AR	5
16.00	20.51	11.43	1.09	0.97	37.21	-22.21	12.62	1.58	1.00	Major	1
20.64	43.25	13.85	1.14	0.99	60.49	-39.65	13.68	1.86	0.99	Major	2
12.35	19.83	7.150	1.00	0.99	30.59	-17.70	11.61	12.0	1.00	Major	3
20.83	30.66	16.87	2.16	0.99	52.13	-30.20	12.75	2.87	1.00	Major	4
21.20	44.95	13.66	1.25	1.00	67.13	-50.19	14.84	1.06	1.00	Major	5

doi:10.1371/journal.pone.0169866.t001

one exception for droplet 3 that could be explained by its smaller size. Moreover in most case the exponent β is close to one corresponding to a process with a single relaxation time [23].

To obtain a statistical evidence of the reversibility and similar trends for droplets, MANOVA and ANOVA tests were applied. Firstly, a MANOVA model is performed in order to analyse the multivariate response or vector of characteristics that summarize the information of each curve. Table 2 shows the obtained results. Observing the p-values corresponding to each factor, and defining a standard signification level equal to 0.05, we can conclude that the “magnitude” and “change of dimension process” are significant factors (p-values < 0.05); their variations produce significant changes in the response, the vector of KWW parameters and, therefore, in the geometric dimension curves related to deformation/relaxation processes involved. Then, the dimension curves are different depending on the measured “magnitude” and the studied “process” (deformation or relaxation, elongation or dimension recovery). In addition, Table 2 shows that the response, the dimension curves and thus the relaxation processes do not depend on the droplets in alginate solution. This result is related to the fact that almost all the particles present a similar initial size.

According to the MANOVA results, the geometrical changes of droplets are different depending on “magnitude” and “process”. But testing if there are differences in the characteristic time of the process is not performed yet. This is the more informative parameter, and the index of the droplets deformation/relaxation reversibility in terms of time. Thus, for

**Table 2. MANOVA table for (a, b, λ<sub>c</sub>, β) response: Df are the degrees of freedom, Pillai represent the value of the statistic for each factor, approx. F is the approximate value for F statistic while p-value is the probability of obtaining a sample farthest from null hypothesis (no relation between factor and multiple response) than the obtained using the present sample. If p-value < 0.05, we suppose that the factor is significant regarding to response.**

	Df	Pillai	approx. F	p-value
Magnitude	2	0.95638	45.821	0.0005084
Droplet	4	0.89450	15.842	0.0899211
Process	1	0.40186	31.913	0.0365152
Residuals	22			

doi:10.1371/journal.pone.0169866.t002

**Table 3. ANOVA table using  $\lambda_c$  as response: Df are the degrees of freedom, Mean Squares are the Sum of Squares divided by the degrees of freedom, F is the value of the statistic test while p-value is the probability of obtaining a sample farthest from null hypothesis (the value of the response is the same for all the levels of the factor) than the obtained using the present sample. If p-value < 0.05, we suppose that the factor is significant with respect to response.**

Factor	Df	Sum of squares	Mean squares	F value	p-value
Magnitude	2	21.86	10.93	1.365	0.2761
Droplet	4	147.3	36.83	4.601	0.0075
Process	1	1.780	1.78	0.0340	0.6417
Residuals	22	176.1	8.00		

doi:10.1371/journal.pone.0169866.t003

completing the analysis of variance, an ANOVA table was then performed using only the characteristic time  $\lambda_c$  as response variable (Table 3). The p-values corresponding to “magnitude” and “process” factors indicate that these factors are not significant in the estimated characteristic time (p-values > 0.05). The characteristic time does not depend neither on the chosen geometrical parameter (AR, area, or major) nor the “process” (deformation or relaxation). Deformation and relaxation are reversible processes in terms of time. Nevertheless, the p-value corresponding to the “particle” factor (p-value < 0.05) indicates that the estimated relaxation time is different depending on the studied droplet at least in one level. In all the statistical tests, the signification coefficient is fixed at 0.05.

The dependence of relaxation time on droplet was studied by implementing a multiple comparison with Tukey test [15]. Table 4 shows the results of multiple comparisons, where “diff” is the difference between the  $\lambda_c$  means of each two compared levels, “lower” is the lower end point of the 95% confidence interval for this difference, “upper” gives the upper end point, and the “adjusted p-value” is the p-value of Tukey test. Observing the p-values column, the smallest droplet 3 is different to the other ones in terms of  $\lambda_c$  (p-values < 0.05 when compared to 4, 5 and 2). It is important to note that this result is in concordance with the trends of the fits obtained in Table 1. The size of the droplet significantly affects to the relaxation time estimations. These results can also be achieved by observing the lower and upper columns: if the zero value is included in the interval, the two droplets have the same value of relaxation time  $\lambda_c$ .

The characteristic time of deformation/relaxation can be estimated from the KWW fits. The use of the boxplot descriptive technique gives a very informative first approximation for studying the position and dispersion of the  $\lambda_c$  parameter (Fig 10). This tool provides the median, first and third quartiles, and the extreme values that represent the limits for the

**Table 4. Table of multiple comparisons obtained applying the Tukey test to the relaxation time  $\lambda_c$ .**

Multiple comparisons between the different levels of Droplets factor				
Comparison of pair of droplets	diff	lower	upper	Adjusted p-value
1–2	1.801	-3.045	6.648	0.803
1–3	-3.232	-8.078	1.615	0.309
1–4	2.719	-2.127	7.565	0.475
1–5	2.527	-2.319	7.373	0.545
2–3	-5.033	-9.879	-0.186	<b>0.039</b>
2–4	-0.918	-5.764	3.929	0.979
2–5	-0.726	-5.572	4.121	0.991
3–4	-5.950	-10.797	-1.104	<b>0.011</b>
3–5	-5.758	-10.605	-0.912	<b>0.015</b>
4–5	-0.192	-5.038	4.654	1.000

doi:10.1371/journal.pone.0169866.t004

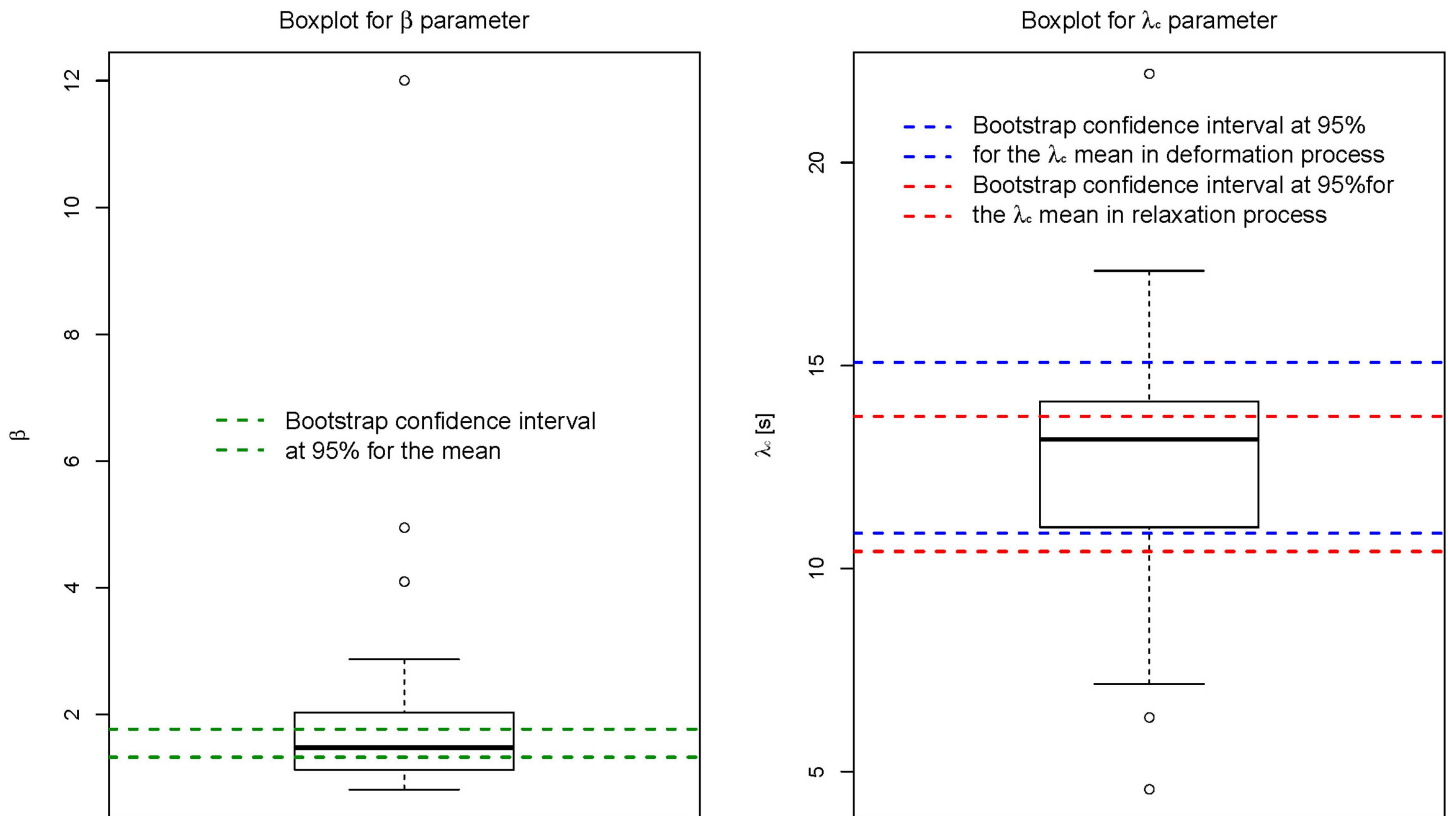


**Fig 10. Boxplots for  $\lambda_c$  and  $\beta$  parameters.** The line in bold represents the median, the inferior and superior edges of the box accounts for the first and third quartiles of the distribution, respectively. The points outside the exterior horizontal lines are defined as outliers.

doi:10.1371/journal.pone.0169866.g010

distribution. The values of  $\lambda_c$  that are out of the (LI, LS) interval are suspected outliers, where  $LS = \max\{x_i; x_i \leq Q_3 + 1.5 \cdot IQ\}$ ,  $LI = \min\{x_i; x_i \geq Q_1 - 1.5 \cdot IQ\}$ ,  $Q_1$  is the first quartile,  $Q_3$  is the third quartile, and IQ is the interquartile range. We also proposed to estimate these characteristic times by using two different confidence intervals at 95% obtained by bootstrap resampling [26] without assuming any parametric assumption (as normal distribution). The confidence intervals for  $\lambda_c$  using the bootstrap R library for the deformation and relaxation are (10.87 s, 15.08 s), and (10.42 s, 13.75 s), respectively. A thousand resamples were used. The intervals are overlapped as above mentioned. This fact support that there are not significant statistical differences between the characteristic time of deformation and the characteristic time of relaxation. There are not evidences to reject the reversibility between deformation and dimension recovery in terms of relaxation time,  $\lambda_c$ .

It is also interesting to estimate the confidence intervals for  $\beta$  parameter that accounts for the number of relaxation processes in a specific material. The confidence limits at a confidence level of 95% obtained for  $\beta$  were (1.33, 1.77), having previously removed the outliers (Fig 9). This is in a good agreement with results obtained from KWW model ( $\beta \sim 1$ ). Monoexponential decay was also observed for the retraction of droplet embedded in an immiscible fluid of same density after a large strain step [27]. It was explained by a reduction of the droplet-matrix interface curvature. In the present study the deformation of droplets is induced by the magnetic field. A bistability model of the shape of a concentrated magnetic droplet under applied magnetic field was developed by Bacri and Salin [28, 29]. These authors have shown that the elongation of a prolate ellipsoidal drop of magnetic permeability  $\mu_2$  in a continuous phase of

permeability  $\mu_1$  (here assumed to be that of vacuum  $\mu_1 \sim \mu_0$ ) results from a balance between the magnetic energy  $E_m$  and the surface energy  $E_s$  which opposes the deformation. When the magnetic field is switched off, the characteristic relaxation time of a spherical droplet is  $\lambda_c = \eta_{eff} R_0 / \sigma$  where  $\eta_{eff}$  is the effective viscosity inside the droplet,  $R_0$  the radius of the spherical droplet and  $\sigma$  is the interfacial tension. Our experimental data are not sufficient to estimate separately  $\eta_{eff}$  and  $\sigma$ . However, the linear relationship between the  $\lambda_c$  parameter for relaxation process and the major diameter of droplets was confirmed by the application of a linear regression model to the pairs of data (see Fig 11). The estimated parametric relationship is  $\lambda_c = 0.852$

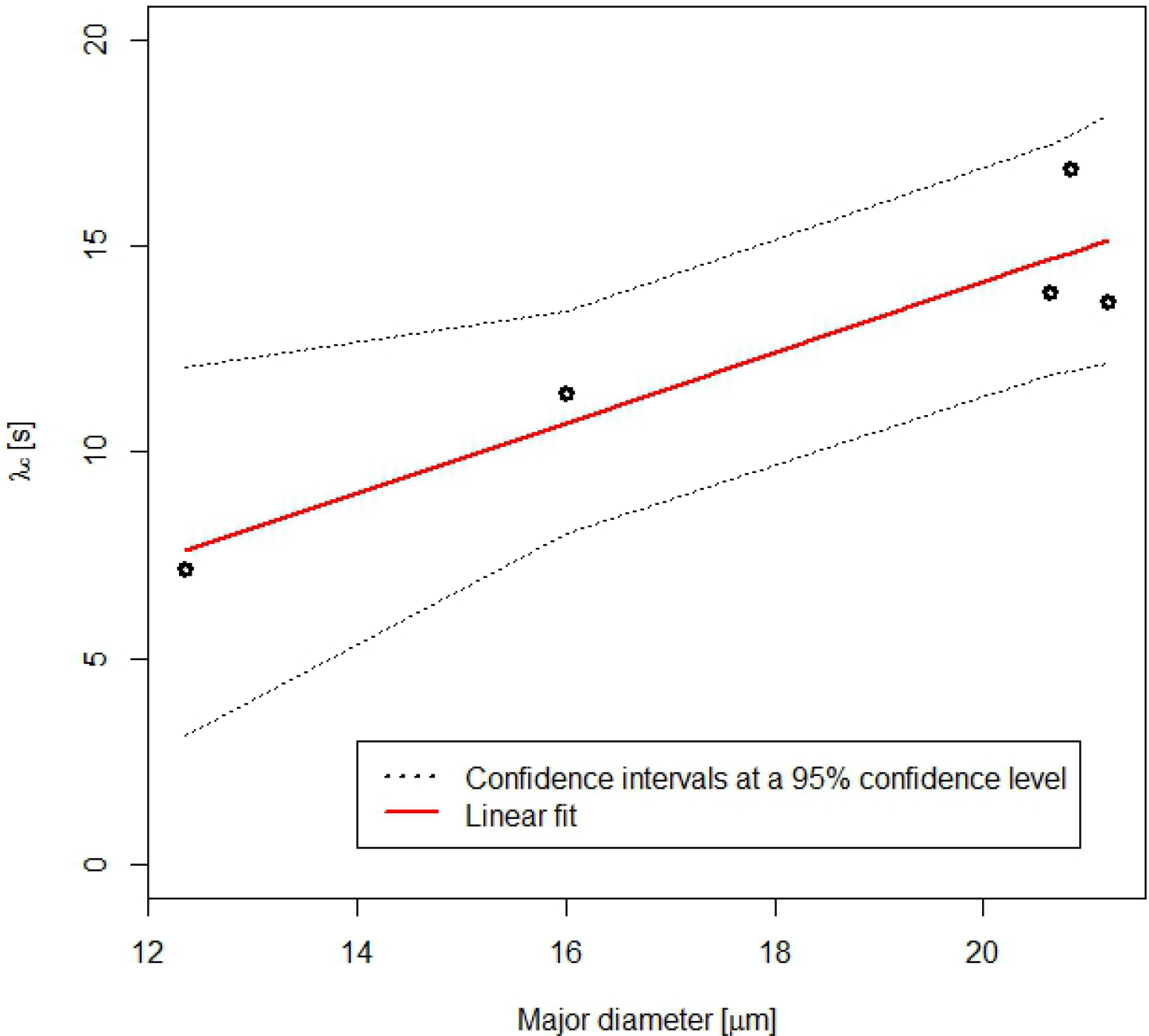


**Fig 11. Relationship between  $\lambda_c$  and the major diameter of the droplets.** Linear fit with 95% confidence levels.

doi:10.1371/journal.pone.0169866.g011

Major diameter due to the intercept is not significant (corresponding p-value greater than any standard signification level). The effect of major diameter on the response  $\lambda_c$  is statistically significant. We have also obtained a relatively high determination coefficient,  $R^2 = 0.85$ , that is a proof of the goodness of fit. This is in accordance with ANOVA results, where  $\lambda_c$  depends on the droplet due to the studied droplets present different sizes. The unexplained variance of the linear model and its relatively wide 95% confidence intervals are due to the uncertainty caused by the enhancement and segmentation processes of the micrographs.

## Conclusions

By using models usually applied to analyze viscoelastic properties, a new testing methodology based on dimensional analysis, image processing, Differential Evolution optimization and nonlinear modeling (Kohlrausch, Williams and Watts model) was successfully proposed to investigate magnetic field induced deformation and relaxation of droplets in an aqueous solution of sodium alginate. Geometrical changes of droplets as a function of time were obtained from the image analysis composed of image enhancement, Mixture Gaussian Modeling segmentation process and parametric regression models. Statistical techniques such as analysis of Variance (ANOVA), Multivariate Analysis of Variance (MANOVA), nonlinear regression and global optimization evolutionary algorithms were applied in order to study transition from ellipsoidal shape of droplet to spherical one as a function of time when magnetic field was switched off.

A characteristic deformation/relaxation time of the droplets in the aqueous solution of sodium alginate was estimated by using two different confidence intervals at 95% for the mean, obtained by bootstrap resampling. It was shown to not globally depend neither on the geometric parameter of the droplet (major diameter, area or ratio of major diameter by minor diameter) nor on the studied process (deformation/relaxation). Otherwise, taking into account the ANOVA results, the characteristic deformation/relaxation time depends on the studied droplet. This fact can be explained by the effect of droplet size.

The obtained values for deformation (10.87 s, 15.08 s) and relaxation (10.42 s, 13.75 s) clearly indicate a reversible magnetic field induced geometrical changes of droplets in aqueous solution of sodium alginate that could be explained by interfacial tension effects as deduced from the linear relationship between the characteristic relaxation time and the major diameter of the droplets.

Finally, the present methodology based on image segmentation and geometrical data modeling, could be applied and extended to other materials with inclusions or nanocomposites materials.

## Author Contributions

**Data curation:** AP.

**Formal analysis:** JTS AP.

**Funding acquisition:** SN.

**Methodology:** CGG AP.

**Project administration:** AP.

**Software:** JTS.

**Supervision:** AP.

**Validation:** JTS AP.

**Writing – original draft:** AP.

**Writing – review & editing:** JTS JLB AP.

## References

1. Tarrío-Saavedra J, López-Beceiro J, Naya S, Gracia C, Artiaga R, Controversial effects of fumed silica on the curing and thermomechanical properties of epoxy composites, *Express Polym. Lett.* 2010; 4:382–95.
2. Ríos-Fachal M, Gracia-Fernández C, López-Beceiro J, Gómez-Barreiro S, Tarrío-Saavedra J, Ponton A. Effect of nanotubes on the thermal stability of polystyrene. *J. Therm Anal Calorim.* 2013; 113:481–7.
3. Tarrío-Saavedra J, López-Beceiro J, Naya S, Artiaga R. Effect of silica content on thermal stability of fumed silica/epoxy composites. *Polymer Degradation and Stability.* 2008; 93:2133–7.
4. Tarrío-Saavedra J, Gracia-Fernández C, López-Beceiro J, Naya S, Artiaga R. TMDSC phase angle for a better nanocomposite interphase identification. *J Therm Anal Calorim.* 2009; 109:1277–84.
5. Schexnailder O, Schmidt G. Nanocomposite polymer hydrogels. *Colloid Polym Sci.* 2009; 287:1–11.
6. Schmidt AM. Thermoresponsive magnetic colloids. *Colloid Polym Sci.* 2007; 285:953–66.
7. Willians G, Watts DC. Non-Symmetrical Dielectric Relaxation Behavior Arising from a Simple Empirical Decay Function. *Trans Faraday Soc.* 1970; 66:80–5.
8. Massart R. Preparation of aqueous magnetic liquids in alkaline and acidic media. *IEEE Trans Magn.* 1981; 17:1247–8.
9. Mallik A, Tarrío-Saavedra J, Francisco-Fernández M, Naya S. Classification of wood micrographs by image segmentation. *Chemometrics Intell Lab Syst.* 2011; 107:351–62.
10. Abramoff MD, Magalhães PJ, Ram Sunanda J. Image processing with ImageJ. *Biophoton Int.* 2004; 11:36–42.
11. R Development Core Team, R: A Language and Environment for Statistical Computing, R Foundation for Statistical Computing, Vienna, Austria, 2014. <http://www.R-project.org>.
12. Tukey JW. *Exploratory Data Analysis*, Addison-Wesley, Reading, MA, 1971.
13. Permuter H, Francos J, Jermyn I. A study of Gaussian mixture models of color and texture features for image classification and segmentation. *Pattern Recognit.* 2006; 39:695–706.
14. Box GE, Hunter JS, Hunter WG. *Statistics for experimenters: design, innovation, and Discovery*, Wiley, second edition, 2005.
15. Maxwell SE, Delaney HD. *Designing experiments and analyzing data. A model comparison perspective*, Lawrence Erlbaum Associates, New Jersey, 2004.
16. Gracia-Fernández C, Tarrío-Saavedra J, López-Beceiro J, Gómez-Barreiro S, Naya S, Artiaga R. Temperature modulation in PDSC for monitoring the curing under pressure. *J Therm Anal Calorim.* 2011; 106:101–7.
17. Artiaga R, López-Beceiro J, Tarrío-Saavedra J, Mier JL, Naya S, Gracia C. Oxidation stability of soy and palm based biodiesels evaluated by pressure differential scanning calorimetry. *ASTM Special Technical Publishing.* 2011; 1477:29–41.
18. López-Beceiro J, Artiaga R, Gracia C, Tarrío-Saavedra J, Naya S, Mier JL. Comparison of olive, corn, soybean and sunflower oils by PDSC. *J Therm Anal. Calorim.* 2011; 104:169–75.
19. Tarrío-Saavedra J, Naya S, Francisco-Fernández M, Artiaga R, Lopez-Beceiro J. Application of functional ANOVA to the study of thermal stability of micro-nano silica epoxy composites. *Chemometrics Intell Lab Syst.* 2011; 105:114–24.
20. Tarrío-Saavedra J, López-Beceiro J, Naya-Fernández S, Gracia-Fernández C, Mier-Buenhombre JL, Artiaga R. Influential factors on the oxidation stability of biodiesel: Statistical study. *Dyna.* 2005; 85:341–50.
21. Anderson TW. *An Introduction to Multivariate Statistical Analysis*, Wiley, 1994.
22. Hand DJ, Taylor CC. *Multivariate Analysis of Variance and Repeated Measures*, Chapman and Hall, 1987.
23. Matsuoka S. *Relaxation phenomena in polymers*, Hanser, Munich, 1992.
24. Storn RM, Price KV, Lampinen JA, *Differential Evolution: a practical approach to global optimization*, Springer-Verlag, Berlin, 2006.
25. Storn RM, Price KV. Differential evolution -a simple and efficient heuristic for global optimization over continuous spaces. *J Glob Optim.* 1997; 11:341–59.



26. Efron B, Tibshirani R. *An Introduction to the Bootstrap*, Chapman and Hall, New York, London, 1993.
27. Assighaou S, Benhyahia L. Universal retraction process of a droplet shape after a large strain jump. *Phys Rev E*. 2008; 77:036305-1–036305-5.
28. Bacrin J-C, Salin D. Instability of ferrofluid magnetic drops under magnetic field. *J Phys Lett-Paris*. 1982; 43:649–54.
29. Bacri J-C, Salin D. Dynamics of the shape transition of a magnetic ferrofluid drop. *J Phys Lett-Paris*. 1983; 44:415–20.